

# Correlation of telomere length shortening with promoter methylation profile of p16/Rb and p53/p21 pathways in breast cancer

Ramin Radpour<sup>1,5</sup>, Zeinab Barekati<sup>1,5</sup>, Mahdi Montazer Haghighi<sup>2</sup>, Corina Kohler<sup>1</sup>, Reza Asadollahi<sup>1</sup>, Peyman Mohammadi Torbati<sup>3</sup>, Wolfgang Holzgreve<sup>4</sup> and Xiao Yan Zhong<sup>1</sup>

<sup>1</sup>Laboratory for Prenatal Medicine and Gynecologic Oncology, Women's Hospital/Department of Biomedicine, University of Basel, Basel, Switzerland; <sup>2</sup>Department of Biology, Faculty of Science, Islamic Azad University, East of Tehran branch, Tehran, Iran; <sup>3</sup>Department of Pathology, Shaheed Beheshti Medical University, Tehran, Iran and <sup>4</sup>Department of Medicine, University Medical Center, Freiburg, Germany

**Unregulated cell growth, a major hallmark of cancer, is coupled with telomere shortening. Measurement of telomere length could provide important information on cell replication and proliferation state in cancer tissues. Telomere shortening and its potential correlation with downregulation of cell-cycle regulatory elements were studied by the examination of relative telomere length and methylation status of the *TP53*, *P21* and *P16* promoters in tissues from breast cancer patients. Telomere length was measured in 104 samples (52 tumors and paired adjacent normal breast tissues) by quantitative PCR. Methylation profile of selected genes was analyzed in all samples using a matrix-assisted laser desorption ionization time-of-flight mass spectrometry (MALDI-TOF MS). Our results demonstrated a significant shortening of tumor telomere regions compared with paired adjacent normal tissues ( $P < 0.001$ ). Similarly, telomere lengths were significantly shorter in advanced stage cases and in those with higher histological grades ( $P < 0.05$ ). Telomere shortening in cancer tissues was correlated with a different level of hypermethylation in the *TP53*, *P21* and *P16* promoters ( $r = -0.33$ ,  $P = 0.001$ ;  $r = -0.70$ ,  $P < 0.0001$  and  $r = -0.71$ ,  $P < 0.0001$ , respectively). The results suggested that inactivation of p16/Rb and/or p53/p21 pathways by hypermethylation may be linked to critical telomere shortening, leading to genome instability and ultimately to malignant transformation. Thus, telomere shortening and promoter hypermethylation of related genes both might serve as breast cancer biomarkers.**

*Modern Pathology* (2010) **23**, 763–772; doi:10.1038/modpathol.2009.195; published online 15 January 2010

**Keywords:** telomere length; breast cancer; biomarker; DNA methylation; MALDI-TOF MS; quantitative real-time PCR

Telomeres are specific repeat sequences (TTAGGG)<sub>n</sub> located at chromosome ends. They have a key role in the maintenance of chromosomal stability.<sup>1</sup> The TTAGGG repeats shorten with each cell division because of end replication mispairing, oxidative damage and other end processing events.<sup>2,3</sup> Tumor cells have extremely short telomeres<sup>4,5</sup> in

association with increased genomic instability.<sup>6,7</sup> This could suggest that telomere changes are implicated in cancer pathways. Similarly, Meeker *et al*<sup>8</sup> observed that telomere length abnormalities occur early in epithelial carcinogenesis. Therefore, telomere length may serve as a useful biomarker in human cancers.

Regulation of p16/Rb and p53/p21 pathways are important proliferation control mechanisms that are linked to telomere shortening in human cells.<sup>9</sup> Inactivation of p53 enables continued proliferation of cells with dysfunctional telomeres, ultimately promoting chromosomal instability and transformation,<sup>10,11</sup> whereas expression of p16 inhibits phosphorylation of the retinoblastoma protein (pRB), thus preventing cell-cycle progression.<sup>12</sup> Recent

Correspondence: Professor XY Zhong, Laboratory for Prenatal Medicine and Gynecologic Oncology, Women's Hospital/Department of Biomedicine, Room No. 420, University of Basel, Hebelstrasse 20, Basel CH 4031, Switzerland.

E-mail: zhongx@uhbs.ch

<sup>5</sup>These authors contributed equally to this work.

Received 31 July 2009; revised and accepted 14 December 2009; published online 15 January 2010

data suggest that the severe genome instability present during telomere crisis, promotes secondary genetic changes that facilitate carcinogenesis.<sup>13,14</sup> Other studies indicated that upregulation of *p16* in senescent cells may also be a consequence of telomere dysfunction.<sup>15</sup>

Optimal telomere length determination is achieved by real-time polymerase chain reaction (PCR).<sup>16</sup> This method relies on the use of telomere primers consisting of a six nucleotide repeated pattern containing four consecutive paired bases, followed by two mismatched bases and a unique 5' sequence. The technique permits calculation of a ratio of telomere repeat copy number to a chosen internal control gene copy number as a relative measure of telomere length unit.

The SEQUENOM's EpiTYPER assay is a methylation quantification method which relies on MALDI-TOF MS.<sup>17</sup> The robustness of this approach for DNA methylation quantification has been previously confirmed by ulterior studies.<sup>18-20</sup> In the current report, this assay was used to quantify the methylation of *TP53*, *P21* and *P16* promoter regions.

The aim of this study was to investigate a potential link between promoter hypermethylation of the *TP53*, *P21* and *P16* genes and telomere length shortening. Paired breast tumor and adjacent normal breast tissues were analyzed by quantitative PCR and MALDI-TOF MS to measure relative telomere length and promoter methylation level of aforementioned genes, respectively. In addition, we compared telomere length in tumor tissues to traditional pathological parameters and clinical predictive markers.

## Materials and methods

### Samples

The study was approved by the local institutional review board. Cases with demonstrated *BRCA1* or *BRCA2* germline mutations or primary invasive breast carcinoma were excluded. Size of each tumor was evaluated by calculation of surface area (in cm<sup>2</sup>) based on the measurement of its two greatest axes. Samples were obtained from 52 paraffin-embedded breast cancer tissues and 52 paired adjacent normal tissues. The corresponding embedded tissue in paraffin blocks of both tumor and adjacent normal tissue were sectioned in 5  $\mu$ m thickness for immunohistochemical staining study. The pathological type, grading and staging were confirmed from the original microscopy slides, which were reviewed separately by two experienced pathologists. Staging and grading was evaluated according to the WHO histological classification.

Remaining part of the paraffin blocks were sectioned (thickness, 10–20  $\mu$ m) from entirely neoplastic and adjacent normal tissue for DNA extraction. Three to five tissue sections (around 100 mg of tissue) were subjected for DNA extraction using

the High Pure PCR Template Preparation Kit (Roche Diagnostics, Mannheim, Germany).

### Immunohistochemical Staining

The standard avidin-biotin-peroxidase-complex and heat-induced antigen retrieval using the microwave method was applied for all immunohistochemical staining. The analysis for the detection of estrogen receptor (ER), progesterone receptor (PR) and HER2/neu (C-ErbB-2) proteins was carried out on 5  $\mu$ m-thick sections of paraffin-embedded tissue blocks using primary antibodies for ER (Dako Ltd, Cambridgeshire, UK; clone ID-5, 1:50 dilution), PR (Dako, clone PgR, 1:300 dilution) and HER2/neu antibody (Dako, clone PN2A, 1:200 dilution). Horseradish peroxidase-streptavidin was added and incubated for 30 min followed by dimethylaminoazobenzene (DAB) treatment for 10 min.

Appropriate positive and negative controls were included with each immunohistochemical staining. Normal breast tissues from the studied cases served as an additional internal control. The Quick Score method was used for semi-quantification of ER and PR status as follows: The slides were assessed for average degree of the staining at low power ( $\times 10$ ), and the following scores were allocated: negative (0), weak (1), moderate (2) or strong (3). The percentage of cells with positive nuclei was counted at high power ( $\times 40$ ), and the following scores were allocated:  $<25\%$  (1),  $25\leq 50\%$  (2),  $50\leq 75\%$  (3) and  $>75\%$  (4). HER2/neu immunoreactivity was scored according to the conventional scoring system as follows: (0) negative, (1+) negative, (2+) equivocal or weakly positive and (3+) strongly positive.

### Quantitative Assessment of the Telomere Length

Telomere repeated sequences and glyceraldehyde-3-phosphate dehydrogenase gene (*GAPDH*) amplification was carried out for each sample by real-time PCR. *GAPDH* was used as internal control (nuclear DNA (nDNA) reference) against which DNA quantification normalization was carried out. Primers were as follows: for *GAPDH*, forward 5'-CCCCACACAC ATGCACTTACC-3' and reverse 5'-CCTAGTCCCA GGGCTTTGATT-3'; for telomere DNA (tDNA), forward 5'-CGGTTTGGTTGGGTTTGGGTTTGGGTTTGGTTTGGGTT-3' and reverse 5'-GGCTTGCCTTACCCTTACCCTTACCCTTACCCT-3'.<sup>16</sup> Detection and quantification were carried out with the ABI Prism 7000 Sequence Detector and ABI Prism 7000 SDS software (Applied Biosystems, Foster City, CA, USA), respectively.

Reaction was carried out with 5  $\mu$ l of template DNA, 12.5  $\mu$ l SYBR Green PCR Master Mix (Applied Biosystems) and 7.5  $\mu$ l of each 10  $\mu$ M primers, for a final reaction volume of 25  $\mu$ l. Thermal cycling was carried out according to the following reaction

sequence: 95 °C for 10 min, followed by 40 cycles of 95 °C for 15 s and 54 °C for 2 min for the telomere amplification, and 95 °C for 10 min, followed by 40 cycles of 95 °C for 15 s and 60 °C for 1 min for *GAPDH*. Following amplification, a dissociation curve was drawn to confirm the specificity of the reaction. Standard and dissociation curves were generated with the ABI Prism 7000 SDS software.  $R^2$  for each standard curve was >0.98.

We examined the amplification efficiency for both *GAPDH* and telomere DNA with a set of serial dilutions, specifying a tDNA and a 97-bp *GAPDH* amplicon concentrations ranging from  $3.125 \times 10^4$  to 10 pg/ $\mu$ l (including 31 250, 6250, 1250, 250, 50 and 10 pg/ $\mu$ l). There was good correlation of tDNA and *GAPDH* signal on serial dilutions, with comparable efficiencies of amplification. The average threshold cycle number (Ct) values of *GAPDH* and tDNA were obtained from each case in this study. The relative telomere length was calculated using the average Ct of telomere DNA and *GAPDH* ( $\Delta C_t = C_t \text{ GAPDH} - C_t \text{ tDNA}$ ) in the same sample as an exponent of 2 ( $2^{\Delta C_t}$ ). All samples were run in parallel triplicate and the median value was used for calculations. In each run, a standard curve and a negative control (water) were included.

#### High-Throughput Methylation Analysis using Thymidine-Specific Cleavage Mass Array on MALDI-TOF Silico-Chip

The EpiTYPER assay using MALDI-TOF MS and MassCLEAVE reagent was assessed for high-throughput analysis of DNA methylation patterns of three tumor suppressor gene promoters (*TP53*, *P21* and *P16*) according to the previously published methods.<sup>17,19–21</sup>

Briefly, bisulfite conversion of the target sequence was obtained using the EpiTect bisulfite kit (QIAGEN AG, Basel, Switzerland). Primers were designed to cover the promoter regions with the most CpG sites. A T7-promoter tag was added to the reverse primer and a 10mer-tag sequence was added to the forward primer to balance the PCR primer length.<sup>20</sup> Unincorporated dNTPs were dephosphorylated by alkaline phosphatase treatment (SAP; SEQUENOM, San Diego, CA, USA). Typically, 2  $\mu$ l of the PCR were directly used as a template in a 5  $\mu$ l of *in vitro* transcription reaction. In all, 20 U of T7 R&DNA polymerase (Epicentre, Madison, WI, USA) was used to incorporate dTTP in the transcripts. Ribonucleotides and dNTPS concentrations were 1 and 2.5 mmol/l, respectively. In the same step, the RNase A (SEQUENOM) was added to cleave the *in vitro* transcript (T-cleavage assay). The mixture was robotically dispensed (nanodispenser) onto silico chips preloaded with matrix (SpectroCHIP; SEQUENOM). Mass spectra were collected using a MassARRAY Compact MALDI-TOF (SEQUENOM) and spectra's methylation ratios

were generated by the EpiTyper software v1.0 (SEQUENOM).

#### Statistical Analysis

Data analysis was carried out using the SPSS software (Statistical Software Package for Windows, version 17). The Shapiro–Wilk and Kolmogorov–Smirnov tests were used to data distribution analysis. Both tests similarly demonstrated that our data set was not normally distributed ( $P = 0.000/0.000$  by Shapiro–Wilk test and  $P = 0.000/0.001$  by Kolmogorov–Smirnov test for tDNA assay and *GAPDH* assay, respectively). The relative telomere length is given as the median. Wilcoxon signed ranks test was used to compare the differences between ranks of each paired samples. The Mann–Whitney *U*-test and Kruskal–Wallis test were used to compare the shortened telomere length in the cancer tissues and paired normal tissues.

Quantitative methylation status of the three previously stated tumor suppressor promoters was compared with relative telomere length. Using the two-way hierarchical cluster analysis, the most variable CpG fragments for each gene were clustered based on pair-wise Euclidean distances and linkage algorithm for all studied samples according to the previously developed method.<sup>19–21</sup> For gene clustering, pair-wise similarity metrics were calculated for each gene separately based on methylation ratio of cancer tissues across the adjacent paired normal tissues. The procedure was carried out using the double dendrogram function of the Gene Expression Statistical System for Microarrays (GESS) version 7.1.19 (NCSS, Kaysville, UT, USA). The non-parametric Spearman's  $\rho$ -test was used for correlation study between telomere length and promoter hypermethylation of *TP53*, *P21* and *P16* gene promoters using SPSS software.

## Results

### Pathological Classification of Samples

According to pathological tumor type and immunohistochemical staining, we separated our patient's samples into two subgroups: ductal carcinoma and lobular carcinoma (Figure 1). Breast cancer characteristics, such as staging, histological grading, hormone receptor status and HER2/neu expression from breast cancer patients are listed in Tables 1 and 2.

### Telomere Length Quantification and Methylation Analysis using Paraffin Embedded Tissues

The use of formalin-fixed, paraffin-embedded tissue sections, for which there is a significant degree of degradation, fragmentation and chemical modification of the nucleic acids, is a major limitation for this type of study<sup>19,22</sup> because it can reduce the

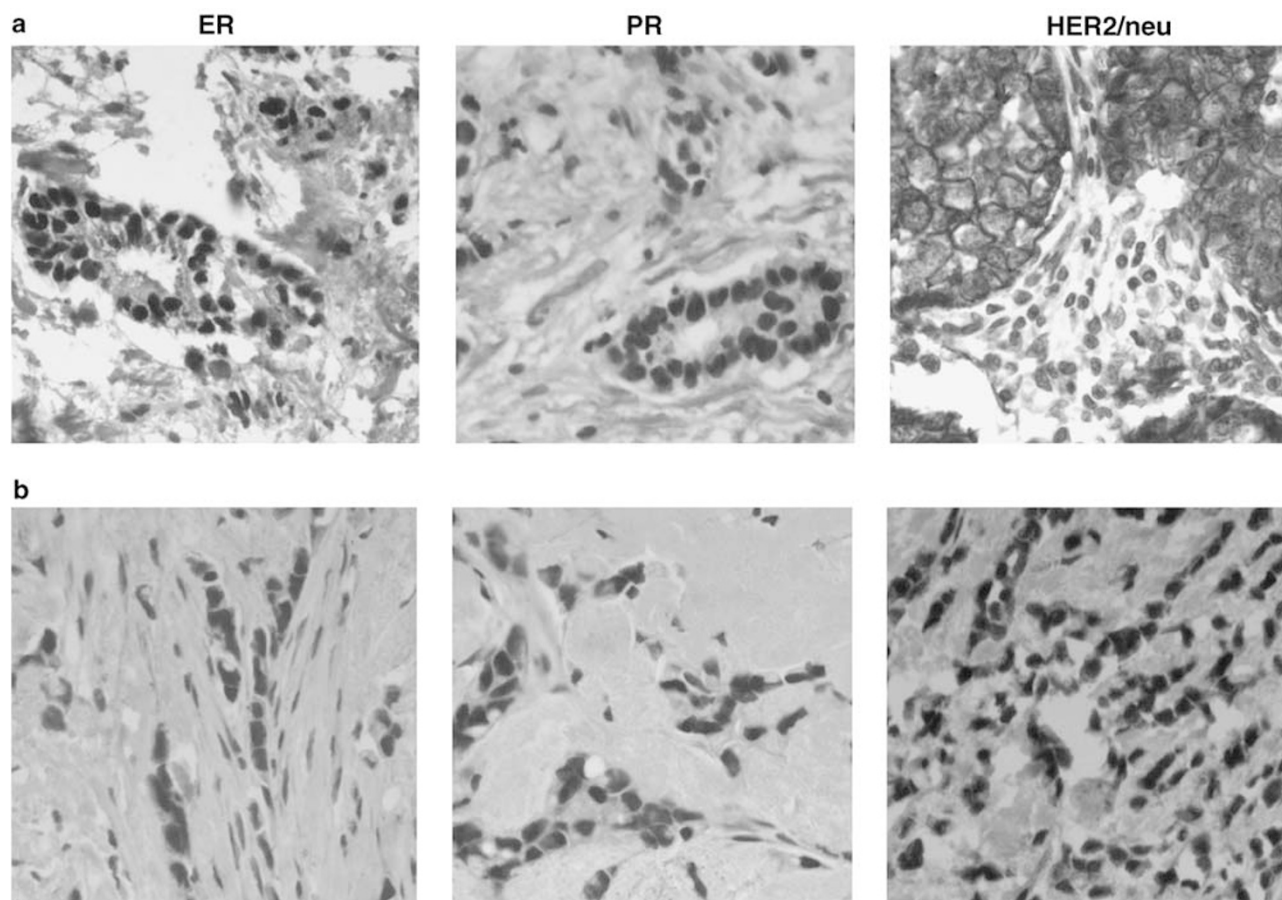


**Figure 1** Immunohistochemical staining for estrogen receptor (ER), progesterone receptor (PR) and HER2/neu proteins. (a) Ductal carcinoma. (b) Lobular carcinoma.

sensitivity of the telomere length measurement.<sup>23,24</sup> In this study, we explored the feasibility of using paraffin-embedded tissues for the quantitative assessment of telomere length together with high-throughput methylation quantification on MALDI-TOF silico-chips.<sup>20,21</sup> Before carrying out telomere length analysis, yield of extracted DNA from formalin-fixed paraffin-embedded tissues was quantified using NanoDrop ND-1000 spectrophotometer (Biolab, Mulgrave, Vic, Australia). Median DNA quantities was determined as 37.92 ng/ $\mu$ l. Samples with <10 ng/ $\mu$ l of DNA were not considered for further experiments and DNA extraction for these samples was repeated.

#### Relative Telomere Length in Cancer and Paired Normal Breast Tissues

Data analysis demonstrates an 8.58 cycle difference ( $\Delta\Delta$ Ct, delta Ct) between normal and cancer tissues. The telomere length in cancer tissues was significantly lower than that in normal tissues (Mann-Whitney *U*-Test:  $P < 0.001$ ) (Figure 2a). Out of 52 paired samples, 41 pairs show telomere length

in normal tissues significantly longer than telomere length in tumors (Wilcoxon signed ranks test:  $P < 0.001$ ).

#### Correlation Between Shortened Telomere Length and Other Prognostic Factors for Breast Cancer

In this study, associations between the ratio of telomere length in breast cancer tissues and traditional clinical parameters, such as age, tumor type, tumor size, lymph node involvement, extent of metastasis, stage, histological grading, receptor status and pathological biomarkers (HER-2/neu and PS2), were analyzed (Table 2). Shortened telomere length in breast cancer tissues was not associated with age ( $\geq 50$  vs  $< 50$ ), tumor type (ductal vs lobular), tumor size (T1, T2 and T3), lymph node involvement (N0 and  $N \geq 1$ ), ER and PR status, HER-2/neu amplification nor presenilin 2 (PS-2) detection (Table 2). However, shorter telomere length was correlated with higher histological grading (grade I vs II and III,  $P = 0.007$ ) (Figure 2c) and distant metastasis ( $P = 0.035$ ) (Figure 3). We could not find any significant telomere length

**Table 1** Clinical characteristics of patient's samples

Breast cancer tumor type	Total no. of patients	Age (years) (mean $\pm$ s.d. (range))	Side of tumor		Tumor size (cm) (mean $\pm$ s.d. (range))	No. of patients with lymph node involvement	No. of patients with metastasis	Histological grade		
			R	L				Grade 1	Grade 2	Grade 3
Ductal carcinoma	41	48 $\pm$ 11.2 (32–78)	19	22	3.6 $\pm$ 3.1 (0.8–12)	33	9	7	15	19
Lobular carcinoma	11	50 $\pm$ 10.9 (32–65)	6	5	3.25 $\pm$ 1.6 (1.5–6)	6	2	3	3	5

**Table 2** Correlation between relative telomere length in cancer tissues and clinical parameters

Variables	Group (cases)	Telomere length (median)	P-value
Age (years)	< 50 (33)	0.069	0.294 <sup>a</sup>
	$\geq$ 50 (19)	0.106	
Histological type	Ductal (41)	0.099	0.491 <sup>a</sup>
	Lobular (10)	0.035	
Primary tumor	T1 (23)	0.069	0.397 <sup>b</sup>
	T2 (16)	0.052	
	T3 (9)	8.439	
Lymph node involvement	Positive (39)	0.069	0.185 <sup>a</sup>
	Negative (13)	0.271	
Distant metastasis	No metastasis (41)	4.291	0.035 <sup>a</sup>
	Metastasis (11)	0.069	
Stage	I (6)	8.439	0.028 <sup>b</sup>
	II (27)	0.541	
	III (8)	1.119	
	IV (11)	0.469	
Histological grading	G1 (10)	2.950	0.07 <sup>b</sup>
	G2 (18)	0.036	
	G3 (24)	0.035	
	Positive (14)	0.271	
ER	Negative (18)	0.036	0.342 <sup>a</sup>
	Positive (18)	0.332	
PR	Negative (14)	0.041	0.138 <sup>a</sup>
	Positive (15)	0.069	
HER2/neu	Negative (17)	0.084	0.664 <sup>a</sup>
	Positive (4)	2.587	
P53	Negative (29)	1.069	0.185 <sup>a</sup>
	Positive (12)	0.114	
PS-2	Positive (20)	0.524	0.836 <sup>a</sup>
	Negative (20)	0.524	

ER, estrogen receptor; PR, progesterone receptor.

<sup>a</sup>Mann–Whitney *U*-test.<sup>b</sup>Kruskal–Wallis test.

changes in the normal samples and their clinical prognostic parameters ( $P > 0.05$ ).

### Methylation Status of Three Tumor Suppressor Genes Using MALDI-TOF MS

The quantitative methylation profile of three tumor suppressor promoters (*TP53*, *P21* and *P16*) was compared with relative telomere length in breast cancer and paired normal tissues. The CpG sites were analyzed by T-cleavage assay using MALDI-TOF MS. For these three studied promoters, we analyzed one amplicon per gene containing 83 CpG sites per sample (4316 CpG sites in total).<sup>20</sup> Using the two-way hierarchical cluster analysis, we demonstrated different levels of methylation in the three studied promoters in cancer and adjacent normal tissues (Figure 4). The results showed significant correlation between the telomere length shortening ratio in cancer tissues and the *TP53*, *P21* and *P16* promoters hypermethylation ( $r = -0.33$ ,  $P = 0.001$ ;  $r = -0.70$ ,  $P < 0.0001$  and  $r = -0.71$ ,  $P < 0.0001$  respectively) (Figure 4).

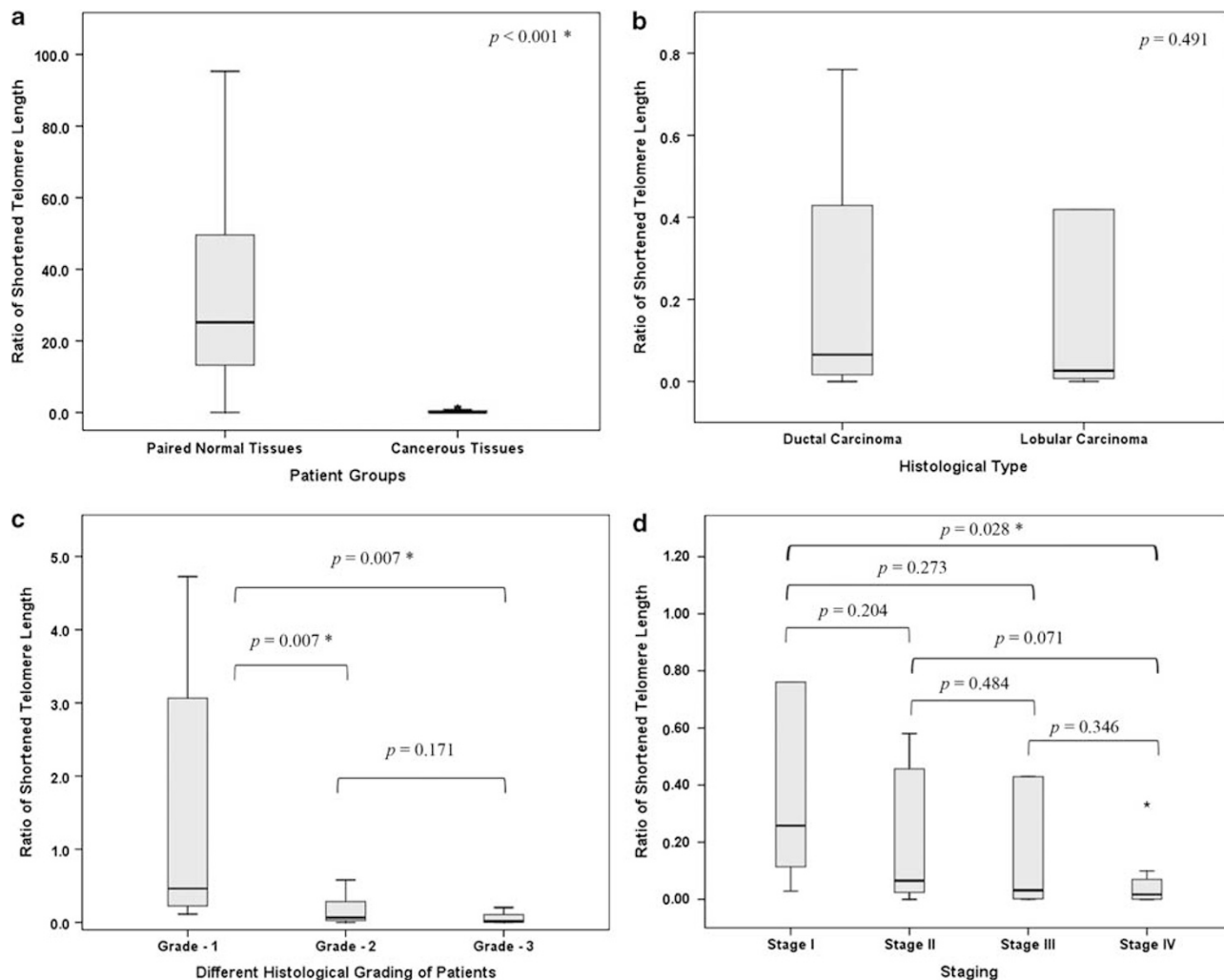


**Figure 2** (a) Telomere length in the 52 breast cancer tissues and 52 paired normal tissues. (b) Telomere length in the two tumor types (ductal carcinoma and lobular carcinoma). (c) Telomere length relative to histological grade. (d) Telomere length relative to staging. (\*significant correlation; Mann–Whitney *U*-test.)

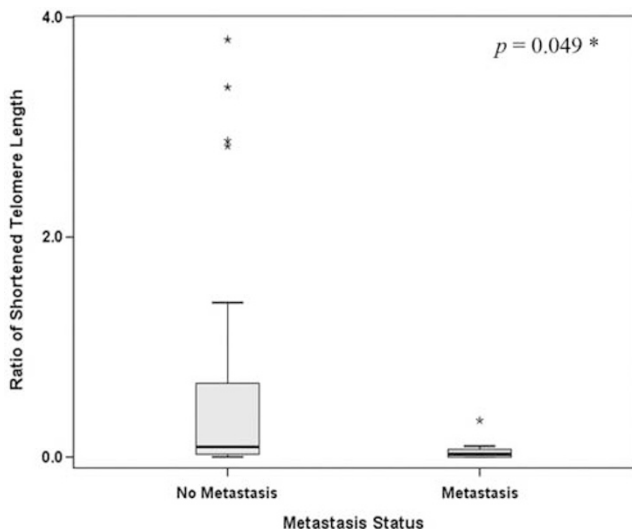


**Figure 3** Telomere length in relation to metastasis status. (\*Mann–Whitney *U*-test.)

## Discussion

The association between telomere length alterations and cancer has been studied for decades. In the present study, telomere length and promoter methylation status of the p16/Rb and p53/p21 pathways were examined in different grades of breast cancer in 104 paired cancer and normal tissues from 52 patients with breast cancer. Our results show that the average telomere length in breast cancer tissue was significantly shorter than that in the adjacent normal tissue, especially in the histological grades II and III ( $P < 0.001$ ) (Figure 2c). Moreover, hypermethylation of *TP53*, *P21* and *P16* promoters significantly correlated with shortened telomere length in the cancer tissues ( $P < 0.001$ ) (Figure 4).

The most important function of telomeres is the maintenance of genomic integrity and stability.<sup>1,25</sup> Recently, Lin *et al*<sup>24</sup> reviewed the dynamics of telomere length in different types of cancers. Several studies examining telomere length in humans found

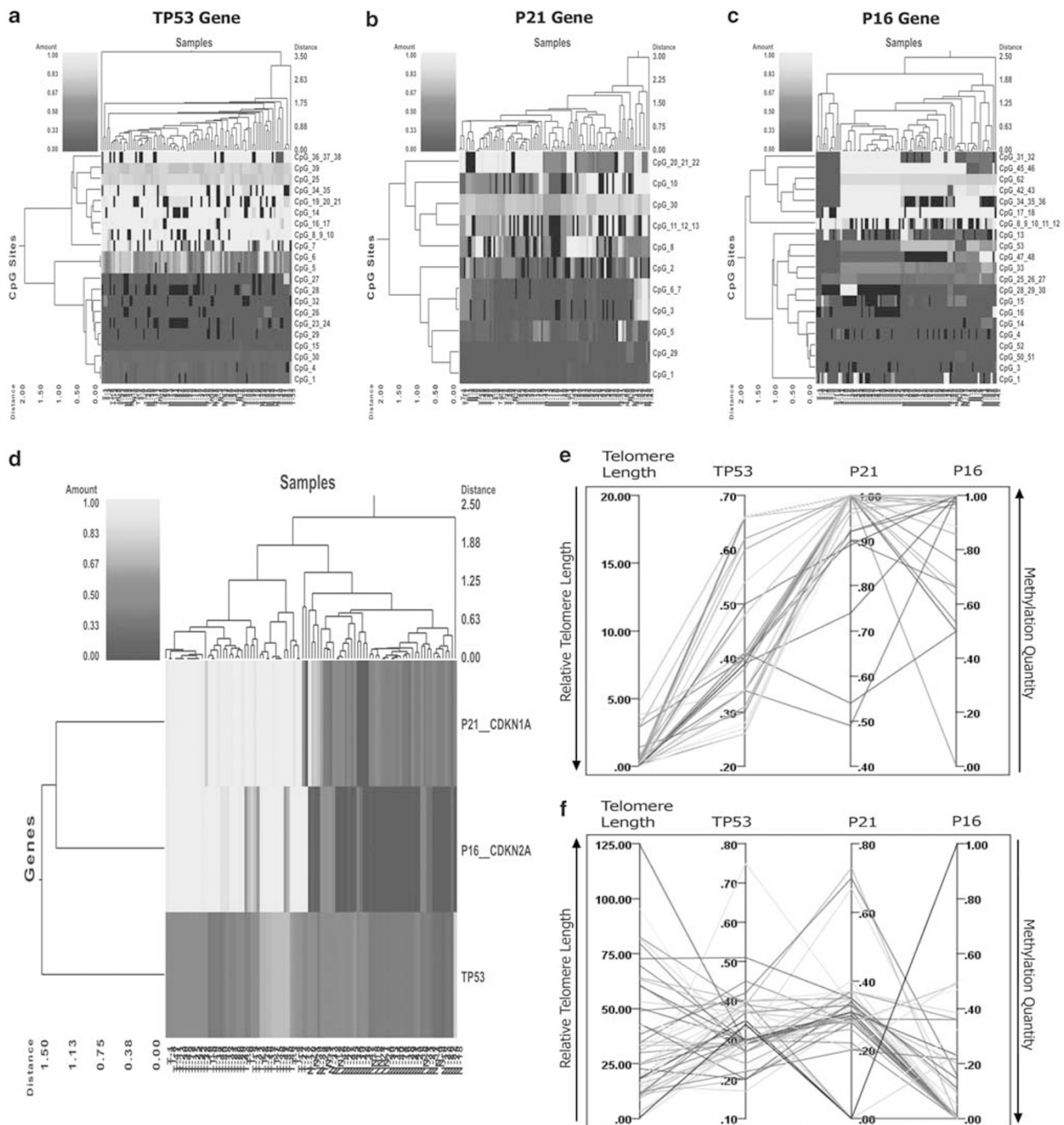


**Figure 4** Correlation study between methylation profile of the three tumor suppressor genes (*TP53*, *P21* and *P16*) in cancerous tissues and paired normal tissues with relative telomere length. (**a–c**) High-throughput methylation analysis of three breast cancer-related genes by two-way hierarchical cluster analysis. Double dendrograms of the informative CpG sites for the paired samples of breast cancer patients. (Red clusters indicate 0% methylated, yellow clusters indicate 100% methylated, color gradient between red and yellow indicates methylation ranging from 0–100 and black clusters indicate CpG sites not analyzed; T: tumor tissue; N: normal tissue). (**d**) Double dendrogram presenting the methylation profiles of three studied genes (*TP53*, *P21* and *P16*). (**e**) Correlation study between relative telomere length with methylation profile of studied genes in the cancerous tissues. (**f**) Correlation study between relative telomere length with methylation profile of studied genes in the normal tissues. For color figure see online version.

that breast carcinomas had shorter telomeres than normal breast tissue, and high grade (grade III of III) invasive carcinomas had shorter telomeres than low grade (grade I) invasive carcinomas.<sup>26</sup> Our study on paired cancer and normal tissues concurs with those

previous reports, and also demonstrates correlation between shortened telomere length and higher histological grading (Figure 2c and d).

Recently, Svenson *et al*<sup>27</sup> showed that telomere length in peripheral blood cells differs between

breast cancer patients and control subjects, and may serve as a significant prognostic biological marker. In general, malignant tumors show shorter telomeres than corresponding normal tissue, and telomere dysfunction has been indicated as a negative prognostic marker in solid tumors, including breast cancer.<sup>28,29</sup>

Telomere shortening in primary human cells leads to replicative senescence, which is regulated in part by effectors in the p16/Rb and/or p53/p21 pathways.<sup>9,11,30</sup> As well, p53/p21-mediated DNA damage signals are elicited by telomere dysfunction. However, there is still considerable debate on the exact role of telomere attrition on the p16 pathway during senescence.

Inhibition of the p16/Rb and/or p53/p21 pathways enables continuous cell division and critical telomere shortening, a phenomenon known as 'telomere crisis'.<sup>15,31</sup> Using the mass spectrometry on MALDI-TOF silico-chips, we determined quantitative methylation changes of *TP53*, *P21* and *P16* promoters in paired cancer and non-tumor samples. *P21* and *P16* promoters have been reported as being strongly hypermethylated in breast cancer tissues, compared with adjacent normal breast tissues.<sup>20</sup> This study shows significant correlation between telomere length shortening and *TP53*, *P21* and *P16* promoters methylation status (*TP53*: $r = -0.33$ ,  $P = 0.001$ ; *P21*: $r = -0.70$ ,  $P < 0.0001$  and *P16*: $r = -0.71$ ,  $P < 0.0001$ ) (Figure 4) in breast cancer tissues. Although our previous study indicated some hypermethylation level of the *TP53* promoter, this hypermethylation level was not significant in breast cancer tissues in comparison with adjacent normal tissues.<sup>20</sup> Our new finding shows a significant correlation between *TP53* hypermethylation and telomere shortening. This suggests that even low level of hypermethylation of *TP53* can influence telomere length shortening. Taken together, these findings could suggest that p16 and p53/p21 may function as a gatekeeper to prevent critical telomere shortening and genome instability.

Changes in telomere length in breast cancer may not be correlated with distant invasion.<sup>32</sup> However, our results showed a significant correlation between telomere length shortening and distant metastasis ( $P < 0.05$ ) (Figure 3). Although we could not find any significant correlation between telomere length and age ( $\geq 50$  vs  $< 50$ ) in cancer tissue (Figure 5a), a significant shortened telomere length was observed in patients over the age of 50 years ( $P < 0.05$ ) (Figure 5b). This finding is in accordance with previous studies on telomere length and aging.<sup>33,34</sup>

It was reported that telomere length is reduced in histologically normal tissues distant at least 1 cm from the adjacent tumor margins.<sup>35</sup> Although the tissue appears normal, it harbors various genetic changes, including telomere dysfunction, that are reflective of the adjacent carcinogenesis process. This seriously complicates the use of histologically normal tissue as control.<sup>35,36</sup> Also examining

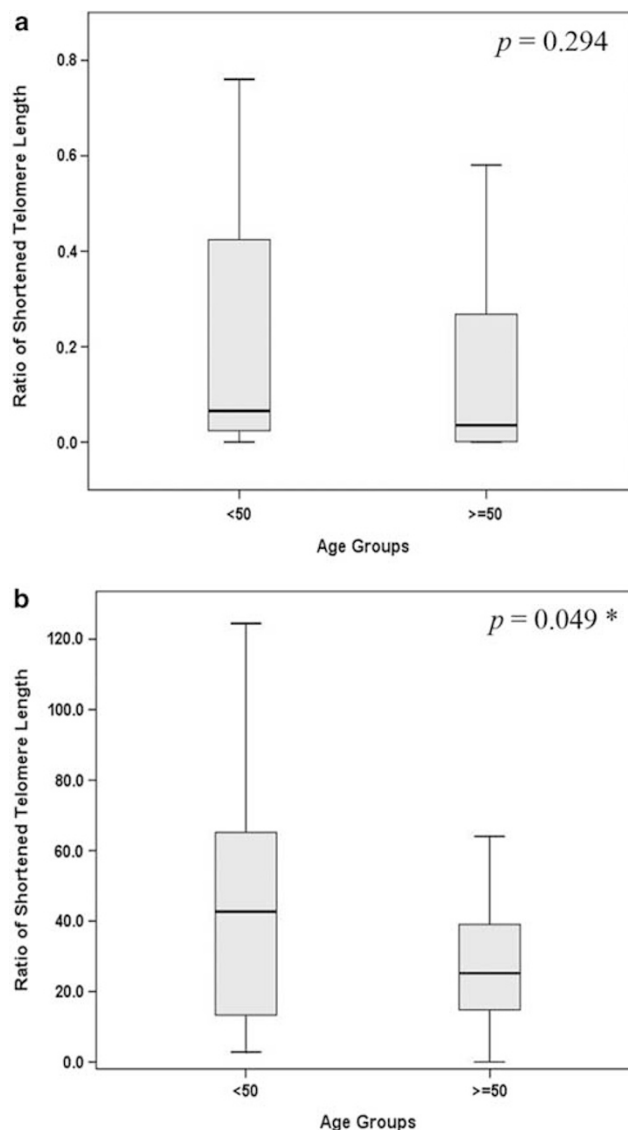


**Figure 5** Comparison of telomere shortening in patient's samples separated according to age, in (a) cancer tissues (b) paired normal tissues. (\*significant correlation; Mann-Whitney *U*-test.)

whole tissue sections rather than examining telomere lengths by *in-situ* methodology, which permits distinction of lesional tissue from contaminating normal tissues is one of the limitations of used methodology.<sup>37</sup> To reduce the challenge of contaminating normal tissues, the paired normal samples in our study were selected with distances more than 1.5 cm to the adjacent tumor tissues. In one report, moderate telomere shortening was observed in approximately 50% of histologically benign breast duct lobular units.<sup>37</sup> This kind of telomere shortening might be the result of physiological proliferation, and may delineate the cells at risk for subsequent malignant transformation, but in our work we could not find significant telomere shortening in the far adjacent normal tissues.



In conclusion, our data suggests that shortened telomere length is significantly correlated with carcinogenesis. Moreover, telomere length is also significantly shorter in cancer tissues from patients with distant metastasis compared with those from patients without metastasis. Promoter hypermethylation of the p16/Rb and p53/p21 pathways showed significant correlation with telomere shortening. The involvement of these cell-cycle regulator pathways may allow for continuous cell division and critical telomere shortening. Shortened telomere length and hypermethylation of p53, p21 and p16 promoters might serve as biomarkers in breast cancer.

## Acknowledgements

We thank Dr Isabelle De Bie for proofreading the text and valuable suggestions also Vivian Kiefer for her help. This work was supported in part by Swiss National Science Foundation (320000-119722/1 and 320030\_124958/1) and Swiss Cancer League, Krebsliga Beider Basel, Dr Hans Altschueler Stiftung, SwissLife and Freiwillige Akademische Gesellschaft (FAK) in Basel, Switzerland.

## Disclosure/conflict of interest

The authors declare no conflict of interest.

## References

- Blackburn EH. Structure and function of telomeres. *Nature* 1991;350:569–573.
- Harley CB. Telomere loss: mitotic clock or genetic time bomb? *Mutat Res* 1991;256:271–282.
- Wright WE, Shay JW. Telomere dynamics in cancer progression and prevention: fundamental differences in human and mouse telomere biology. *Nat Med* 2000;6:849–851.
- Kim NW, Piatyszek MA, Prowse KR, *et al*. Specific association of human telomerase activity with immortal cells and cancer. *Science* 1994;266:2011–2015.
- Shay JW. Telomerase therapeutics: telomeres recognized as a DNA damage signal: commentary re: K. Kraemer *et al.*, antisense-mediated hTERT inhibition specifically reduces the growth of human bladder cancer cells. *Clin. Cancer Res.*, 9: 3794–3800, 2003. *Clin Cancer Res* 2003;9(10 Pt 1):3521–3525.
- Hahn WC. Role of telomeres and telomerase in the pathogenesis of human cancer. *J Clin Oncol* 2003;21:2034–2043.
- Harley CB. Telomerase and cancer therapeutics. *Nat Rev Cancer* 2008;8:167–179.
- Meeker AK, Hicks JL, Iacobuzio-Donahue CA, *et al*. Telomere length abnormalities occur early in the initiation of epithelial carcinogenesis. *Clin Cancer Res* 2004;10:3317–3326.
- Ohtani N, Yamakoshi K, Takahashi A, *et al*. The p16INK4a-RB pathway: molecular link between cellular senescence and tumor suppression. *J Med Invest* 2004;51:146–153.
- Chin L, Artandi SE, Shen Q, *et al*. p53 deficiency rescues the adverse effects of telomere loss and cooperates with telomere dysfunction to accelerate carcinogenesis. *Cell* 1999;97:527–538.
- Artandi SE, Chang S, Lee SL, *et al*. Telomere dysfunction promotes non-reciprocal translocations and epithelial cancers in mice. *Nature* 2000;406:641–645.
- Ben-Porath I, Weinberg RA. The signals and pathways activating cellular senescence. *Int J Biochem Cell Biol* 2005;37:961–976.
- Zhang A, Wang J, Zheng B, *et al*. Telomere attrition predominantly occurs in precursor lesions during *in vivo* carcinogenic process of the uterine cervix. *Oncogene* 2004;23:7441–7447.
- Gisselsson D, Jonson T, Petersen A, *et al*. Telomere dysfunction triggers extensive DNA fragmentation and evolution of complex chromosome abnormalities in human malignant tumors. *Proc Natl Acad Sci USA* 2001;98:12683–12688.
- Jacobs JJ, de Lange T. Significant role for p16INK4a in p53-independent telomere-directed senescence. *Curr Biol* 2004;14:2302–2308.
- Cawthon RM. Telomere measurement by quantitative PCR. *Nucleic Acids Res* 2002;30:e47.
- Ehrich M, Nelson MR, Stanssens P, *et al*. Quantitative high-throughput analysis of DNA methylation patterns by base-specific cleavage and mass spectrometry. *Proc Natl Acad Sci USA* 2005;102:15785–15790.
- Ehrich M, Turner J, Gibbs P, *et al*. Cytosine methylation profiling of cancer cell lines. *Proc Natl Acad Sci USA* 2008;105:4844–4849.
- Radpour R, Haghghi MM, Fan AX, *et al*. High-throughput hacking of the methylation patterns in breast cancer by *in vitro* transcription and thymidine-specific cleavage mass array on MALDI-TOF silico-chip. *Mol Cancer Res* 2008;6:1702–1709.
- Radpour R, Kohler C, Montazer Haghghi M, *et al*. Methylation profiles of 22 candidate genes in breast cancer using high-throughput MALDI-TOF mass array. *Oncogene* 2009;28:2969–2978.
- Radpour R, Sikora M, Grussenmeyer T, *et al*. Simultaneous isolation of DNA, RNA, and proteins for genetic, epigenetic, transcriptomic, and proteomic analysis. *J Proteome Res* 2009;8:5264–5274.
- Srinivasan M, Sedmak D, Jewell S. Effect of fixatives and tissue processing on the content and integrity of nucleic acids. *Am J Pathol* 2002;161:1961–1971.
- Saldanha SN, Andrews LG, Tollefsbol TO. Assessment of telomere length and factors that contribute to its stability. *Eur J Biochem* 2003;270:389–403.
- Lin KW, Yan J. The telomere length dynamic and methods of its assessment. *J Cell Mol Med* 2005;9:977–989.
- Zakian VA. Telomeres: beginning to understand the end. *Science* 1995;270:1601–1607.
- Rha SY, Park KH, Kim TS, *et al*. Changes of telomerase and telomere lengths in paired normal and cancer tissues of breast. *Int J Oncol* 1999;15:839–845.
- Svenson U, Nordfjall K, Stegmayer B, *et al*. Breast cancer survival is associated with telomere length in peripheral blood cells. *Cancer Res* 2008;68:3618–3623.
- Bisoffi M, Heaphy CM, Griffith JK. Telomeres: prognostic markers for solid tumors. *Int J Cancer* 2006;119:2255–2260.
- Heaphy CM, Baumgartner KB, Bisoffi M, *et al*. Telomere DNA content predicts breast cancer-free survival interval. *Clin Cancer Res* 2007;13:7037–7043.

- 30 Kiyono T, Foster SA, Koop JI, *et al*. Both Rb/p16INK4a inactivation and telomerase activity are required to immortalize human epithelial cells. *Nature* 1998;396:84–88.
- 31 Herbig U, Jobling WA, Chen BP, *et al*. Telomere shortening triggers senescence of human cells through a pathway involving ATM, p53, and p21(CIP1), but not p16(INK4a). *Mol Cell* 2004;14:501–513.
- 32 Mambo E, Chatterjee A, Xing M, *et al*. Tumor-specific changes in mtDNA content in human cancer. *Int J Cancer* 2005;116:920–924.
- 33 Aubert G, Lansdorp PM. Telomeres and aging. *Physiol Rev* 2008;88:557–579.
- 34 Blasco MA. Telomeres and human disease: ageing, cancer and beyond. *Nat Rev Genet* 2005;6:611–622.
- 35 Heaphy CM, Bisoffi M, Fordyce CA, *et al*. Telomere DNA content and allelic imbalance demonstrate field cancerization in histologically normal tissue adjacent to breast tumors. *Int J Cancer* 2006;119:108–116.
- 36 Dakubo GD, Jakupciak JP, Birch-Machin MA, *et al*. Clinical implications and utility of field cancerization. *Cancer Cell Int* 2007;7:2.
- 37 Meeker AK, Hicks JL, Gabrielson E, *et al*. Telomere shortening occurs in subsets of normal breast epithelium as well as *in situ* and invasive carcinoma. *Am J Pathol* 2004;164:925–935.